Cell, Vol. 109, 425–436, May 17, 2002, Copyright ©2002 by Cell Press

Path of DNA within the Mu Transpososome: Transposase Interactions Bridging Two Mu Ends and the Enhancer Trap Five DNA Supercoils

Shailja Pathania, Makkuni Jayaram, and Rasika M. Harshey[1]

Section of Molecular Genetics and Microbiology and Institute of Cellular and Molecular Biology
University of Texas at Austin
Austin, Texas 78712

Summary

The phage Mu transpososome is assembled by interactions of transposase subunits with the left (L) and right (R) ends of Mu and an enhancer (E) located in between. A metastable three-site complex LER progresses into a more stable type 0 complex in which a tetrameric transposase is poised for DNA cleavage. "Difference topology" has revealed five trapped negative supercoils within type 0, three contributed by crossings of E with L and R, and two by crossings of L with R. This is the most complex DNA arrangement seen to date within a recombination synapse. Contrary to the prevailing notion, the enhancer appears not to be released immediately following type 0 assembly. Difference topology provides a simple method for determining the ordered sequestration of DNA segments within nucleoprotein assemblies.

Introduction

Biologically important DNA transactions such as replication, segregation, transcription, and recombination are often carried out by elaborate DNA-protein assemblies, whose architecture is derived from specific DNA-protein and protein-protein interactions. In several of these stereospecific high-order complexes, noncontiguous DNA sites have to be brought into proximity by looping, writhing, or branching. Examples include transcriptional enhancesosomes (Schleif, 1992; Tahirov et al., 2002; Tjian and Maniatis, 1994), replisomes (Matthews, 1992), and transpososomes (Chaconas and Harshey, 2002; Chalmers et al., 1998), as well as complexes formed during DNA repair (Ristic et al., 2001), chromosome condensation (Hirano, 2000; Holmes and Cozzarelli, 2000), or DNA cleavage by certain restriction enzymes (Halford, 2001). As a consequence of the multiplicity of precise molecular interactions, the DNA within a given reaction complex is likely restricted to a fixed geometric path. In the absence of DNA-protein cocrystal structures, it is nearly impossible to decipher the precise topology imposed on a DNA substrate by the cognate protein machine that acts upon it. The analysis of the Mu transpososome we present here opens the door to probing these other complex systems by a similar strategy.

Analytical methods for deducing DNA topology have been so far limited to site-specific recombination systems that yield unique inversion or deletion products. In reactions catalyzed by the γδ or Tn3 resolvase protein, the Mu Gin protein/the *Salmonella* Hin protein and the *Escherichia coli* XerC/XerD proteins, synaptic topologies have been arrived at by mapping the number and sign of knot or catenane crossings trapped in the corresponding reaction products (Colloms et al., 1997; Grindley, 1994; Heichman et al., 1991; Kanaar et al., 1990; Stark et al., 1992; Wasserman and Cozzarelli, 1985). These recombinases utilize only circular supercoiled DNA substrates containing a pair of target sites in the appropriate relative orientation, head to head or head to tail. They act on specific phosphate positions, employ transesterification chemistry to mediate DNA breakage and joining, and yield products with complete conservation of the number of phosphodiester bonds present in the substrate. Thus, the topological analysis of these well-behaved recombinases is reasonably straightforward. It has been established that the resolvase and XerC/XerD proteins trap three plectonemic supercoil nodes in their synaptic structures, whereas the Gin (or the Hin) protein traps two such nodes.

By contrast to the site-specific recombination reactions described above, phage Mu transposition, which also requires supercoiling of the substrate and is exquisitely sensitive to the orientation of Mu L and R ends (attL and attR), is not readily amenable to the topological strategy described above. Strand breaking by the transposase protein (MuA) is hydrolytic, and the subsequent promiscuous joining reaction leads to a topologically complex mixture of strand transfer products (Chaconas and Harshey, 2002; Mizuuchi, 1992). We have solved this problem by coupling the complex DNA-protein assembly of the Mu transposition synapse to a simple site-specific recombination reaction carried out by the Cre protein of phage P1, and analyzing the topology of the resulting products. The recombination reaction is used here as a tool for sealing off the synaptic nodes without the possibility of escape.

The rationale for the experimental strategy employed in this study was provided by the previous analyses of recombination carried out by the site-specific recombinases Cre and Flp (encoded by the yeast 2 micron plasmid) from hybrid synapses assembled with the assistance of Tn3 resolvase (Grainge et al., 2000; Kilbride et al., 1999). The topological outcomes were consistent with an antiparallel alignment of the recombination sites and the absence of DNA crossing during the strand exchange reaction per se. In principle, the above geometry and topology (assuming that they are invariant) can be applied to derive the topology of any uncharacterized synapse. In practice, the synapse would be arranged first, Cre (or Flp) recombination would then be carried out, and the DNA crossings in the resulting products analyzed. The topology of the synapse of interest is readily obtained by subtracting from the final product topology the topological contribution made by Cre (or Flp) to the reaction. Further details are given under Results.

Assembly of the Mu transposition complex (the trans-

[1]Correspondence: rasika@uts.cc.utexas.edu

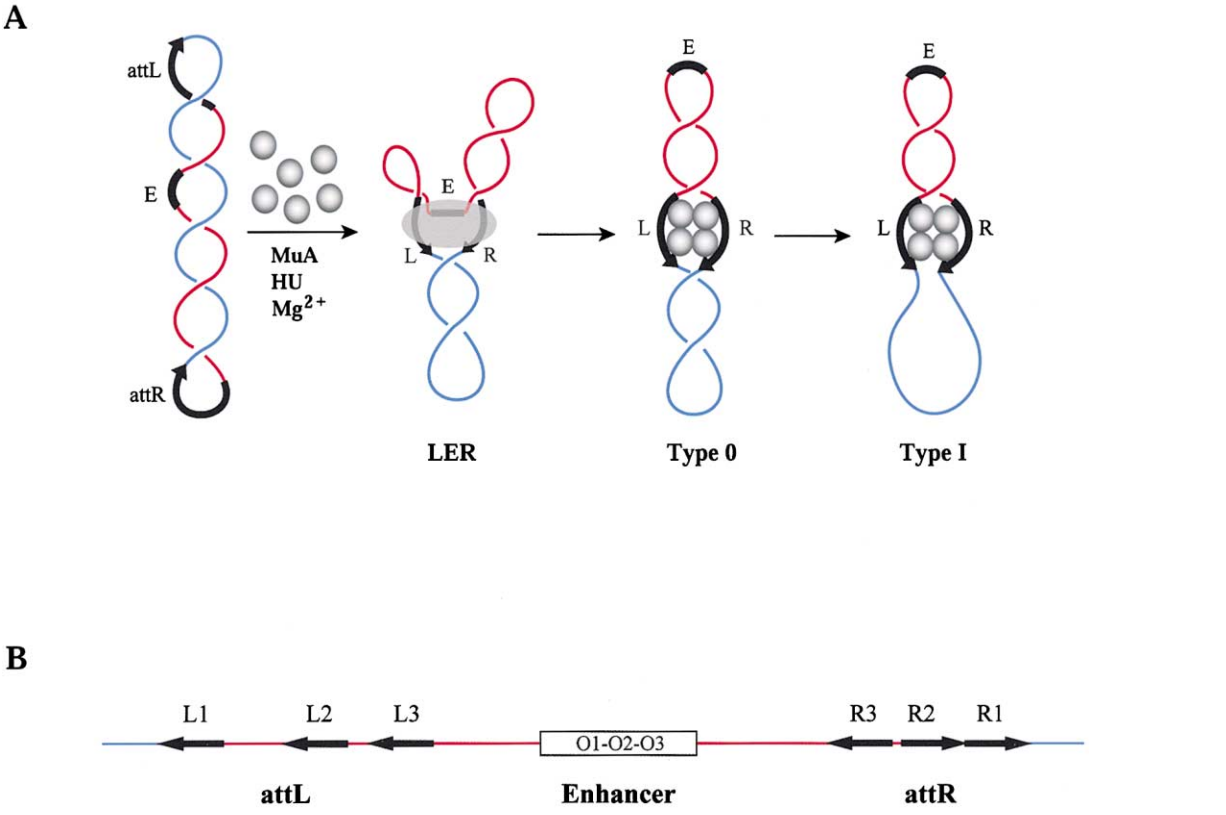

Figure 1. Nucleoprotein assemblies in the cleavage of Mu ends

(A) Interaction between MuA and the attL (L), attR (R), and enhancer (E) sequences triggers transpososome assembly in the presence of the *E. coli* protein HU and divalent metal ions. Assembly proceeds sequentially from the LER complex, through type 0 to the type I complex. The pathway stops at LER when attL and attR contain appropriate mutations (Watson and Chaconas, 1996). The type 0 complex can be trapped in the presence of MuA and Ca^{2+} (Mizuuchi et al., 1992) or the catalytically inactive variant MuA(E392A) (Kim et al., 1995) and divalent metal ions.

(B) Mu ends attL and attR can be divided into three subsites each, L1, L2, and L3 and R1, R2, and R3. In the Mu genome, attL and attR are in head to head orientation. The enhancer, located between attL and attR, overlaps the operators O1-O3.

pososome) requires the head to head orientation of attL and attR in a negatively supercoiled substrate, an enhancer DNA element (E) that normally acts in *cis* with respect to attL and attR (but can also act in *trans* at high concentrations), the MuA protein, the *Escherichia coli* HU protein, and divalent cations (Figure 1; Chaconas and Harshey, 2002). The MuA protein has two distinct DNA binding specificities, one for the att sites and the other for the enhancer. The enhancer plays a dual role in phage Mu physiology. Originally mapped as the operator region to which the Mu repressor binds to regulate lysogeny/lysis (see Chaconas and Harshey, 2002), the enhancer is also required for the prechemical steps of transposition (Figure 1). Maturation of the transpososome proceeds from a metastable LER complex, via the more stable type 0 complex in which MuA has assumed its active tetrameric configuration, to the highly stable type I complex in which strand nicking has occurred at attL and attR. Strand transfer of the cleaved Mu ends to target DNA results in the most stable type II complex (not shown in Figure 1). Even after strand cleavage within the type I complex, the Mu DNA remains supercoiled, anchored by the MuA tetramer, while the non-Mu DNA is relaxed. The schema in Figure 1 reflects the current view that the enhancer-MuA association is transient and is relevant only to the pre-type 0 state (Mizuuchi et al., 1992; Watson and Chaconas, 1996).

We describe here experiments that establish the topology of the LER and type 0 synapses, and show that the enhancer remains associated with the type 0 transpososome. The analysis is complicated by the fact that these synapses involve three DNA domains—the two att sites and the enhancer. Difference topology can only provide information on the number of crossings between two DNA domains separated by the target sites of the recombinase employed in the assay. Hence, we divided the analysis into three separate assays in which the sites were split into binary combinations: enhancer/attL-attR, attL/enhancer-attR, and attR/enhancer-attL. We also performed a fourth assay in which the binary sites were attL/attR, and the enhancer was provided in *trans* and thus topologically unlinked from the reaction. When results from all four assays are combined, a composite picture of the three-site synapse harboring a total of five DNA crossings emerges. The fact that the topological outcome from any one assay is completely consistent

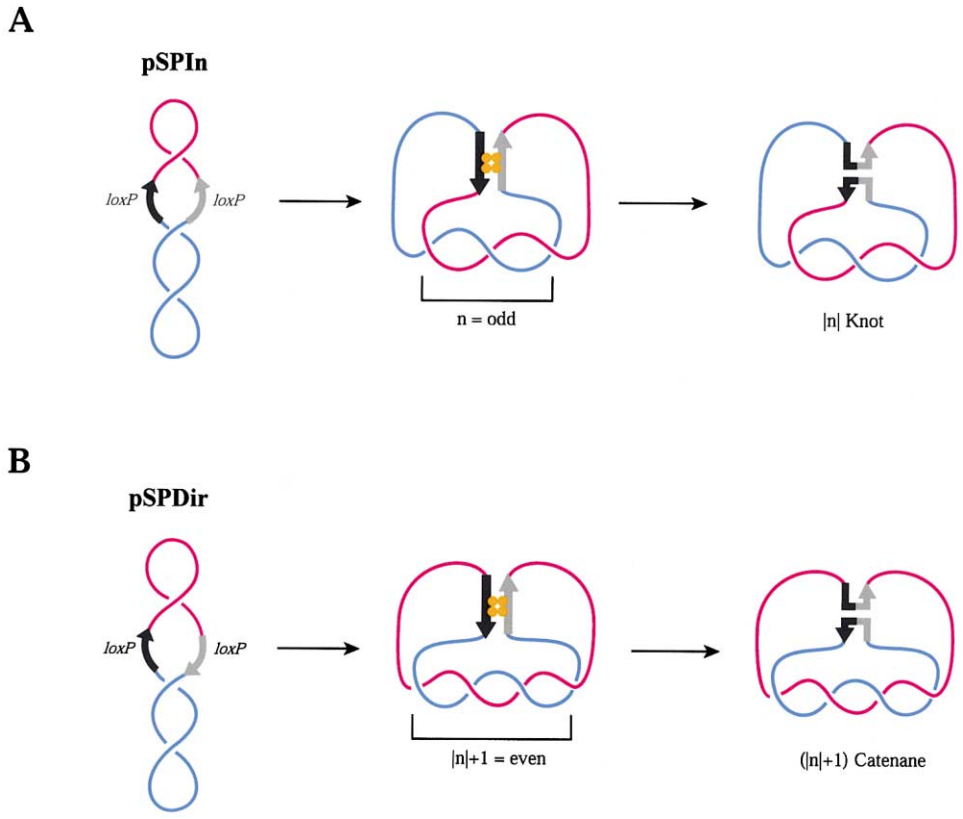

Figure 2. Cre Recombination from a Preassembled Synapse

(A and B) Topological consequences of DNA inversion in pSPIn and deletion in pSPDir by Cre recombination from a preassembled synapse containing n interdomainal superhelical crossings are schematically represented. The location of the Cre reaction is such that the DNA nodes formed within the synapse are preserved in the recombination product.

with those from the other three validates the five-noded, three-site transposition synapse.

Results

The Difference Topology Assay

The logic of the difference topology method for mapping the DNA organization within a DNA-protein synapse of unknown architecture is illustrated in Figure 2. In the two plasmid substrates pSPIn and pSPDir (Figures 2A and 2B), the *loxP* sites (the targets for the Cre protein) are in inverted (head to head) and direct (head to tail) orientations, respectively. They divide each plasmid into two domains shown in red and blue. Recombination mediated by the Cre tetramer would yield a DNA inversion product with pSPIn and a pair of deletion circles with pSPDir. Within the Cre synapse, the partner *loxP* sites are essentially planar (Guo et al., 1997); and, as noted earlier, strand exchange from these sites (related by antiparallel geometry) proceeds without introducing a DNA crossing (Grainge et al., 2000; Guo et al., 1997; Kilbride et al., 1999).

In a general case, if n interdomainal supercoil nodes (n being odd) were trapped in the unknown synapse, inversion by Cre would result in a DNA knot with n crossings (Figure 2A). Notice that an odd number of trapped nodes would arrange the *loxP* sites of pSPIn in antiparallel alignment. For the Cre deletion reaction in pSPDir (Figure 2B), an additional node ($|n| + 1 =$ even) has to be introduced for the antiparallel arrangement of the *loxP* sites. The products of deletion would be a pair of catenated circles linked by ($|n| + 1$) crossings. These nodes are preserved in the recombination products, and report on the DNA topology within the synapse. The location of the *loxP* sites in these plasmids is such that the hybrid synapse (the unknown n synapse with the Cre synapse superposed on it) has very little chance of accidentally acquiring interdomainal nodes $> |n|$ or ($|n|+1$), depending on the *loxP* orientation.

Cre Recombination Following the Assembly of the LER Synapse or the Type 0 Synapse Yields Topologically Complex Products

We now describe the application of difference topology in the analysis of the pretransposition synapses, LER and type 0, with respect to the number of crossings the enhancer makes with the attL and attR DNA. The enhancer is part of a three-site synapse in the LER complex (Watson and Chaconas, 1996), and is thought to be out of the complex in the type 0 transpososome (Mizuuchi et al., 1992; Watson and Chaconas, 1996; see Figure 1). In the plasmid substrates assembled for the assay, pSPIn and pSPDir (see Figure 3), the attL-attR domain (shown in blue) was segregated from the en-

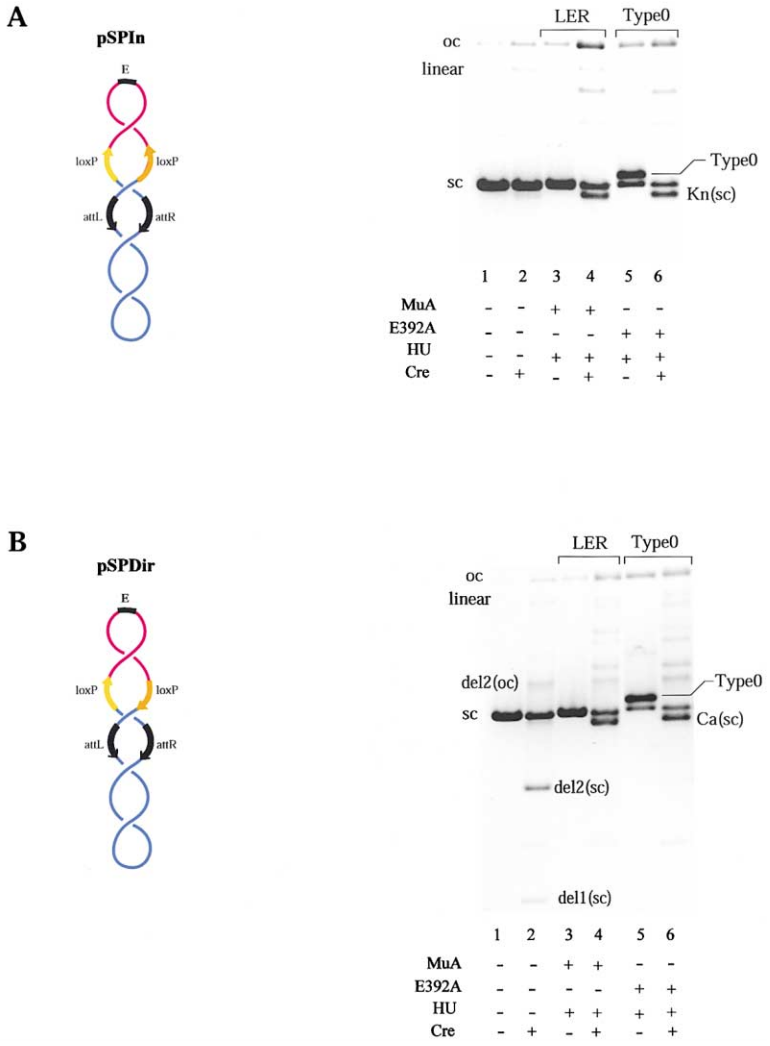

Figure 3. Products of Cre Recombination from Transpososome Assemblies Formed by att-Enhancer-MuA Interactions

In both (A) and (B), lane 1, substrate alone; lane 2, Cre alone reaction; lane 3, assembly of the LER complex; lane 4, Cre recombination from preassembled LER; lane 5, assembly of the type 0 complex; and lane 6, Cre recombination from preassembled type 0. Samples in lanes 2, 4, and 6 were deproteinized prior to electrophoresis. The supercoiled and open circular forms of pSPIn and pSPDir are indicated as sc and oc, respectively. The deletion circles resulting from pSPDir by Cre recombination are denoted by del1 and del2 (sc, supercoiled; oc, open circular). The supercoiled inversion and deletion products from LER or type 0 are labeled Kn (sc) and Ca (sc), respectively.

hancer domain (shown in red) with two *loxP* sites marking their borders. Under these boundary conditions, Cre recombination is expected to reveal the number of crossings between the enhancer and the two att sites combined (red × blue). However, recombination will not disclose the crossings, if any, formed between attL and attR (blue × blue).

In pSPIn and pSPDir, the spatial dispositions of attL, attR, the enhancer element, and the two *loxP* sites (except for their relative orientations) were essentially the same (Figures 3A and 3B). The distance between an att site and its *loxP* neighbor (measured from the end of the L3 or R3 subsite in attL and attR, respectively, to the center of the proximal *loxP* site) was designed to be less than 200 bp to minimize the trapping of random supercoils during Cre recombination from the transpososome-Cre hybrid synapse. At the native plasmid superhelical density of approximately −0.06, one negative DNA crossing exists on average for about 180 bp of DNA (roughly 17 turns). With the present DNA spacings, the contribution of random supercoils to recombination topology must be quite infrequent, and the number of such supercoils cannot be more than one or two. This expectation is borne out by the experimental data. The attR-*loxP* spacing was 165 bp for both pSPIn and pSPDir; the attL-*loxP* spacing was 140 bp for pSPIn and 102 bp for pSPDir. The type 0 complex was assembled in pSPIn and pSPDir using the catalytically inactive MuA(E392A) (Kim et al., 1995). The LER complex was obtained with wild-type MuA and pSPIn and pSPDir variants containing point mutations at the cleavage sites in attL and attR (Watson and Chaconas, 1996).

Roughly 70%–80% of the input pSPIn and pSPDir could be converted to the type 0 complex, which migrated just above the supercoiled substrate during electrophoresis (lane 5, in both Figures 3A and 3B). The extent of the LER complex formed could not be estimated directly because of its instability during gel electrophoresis. We reason that the yield of LER was also similar to that of type 0, as judged by the level of the complex recombination product derived from it upon treatment with Cre (lane 4, in both Figures 3A and 3B; also see below). We have, in addition, confirmed LER formation by stabilizing it via glutaraldehyde crosslinking (Watson and Chaconas, 1996) prior to electrophoresis (data not shown). Inversion or deletion reaction by Cre following LER or type 0 assembly gave products that migrated slightly faster than the supercoiled plasmids

(lanes 4 and 6, Figures 3A and 3B). As revealed by further analyses, these recombinants consisted of supercoiled DNA knots (Kn) for pSPIn, and supercoiled DNA catenanes (Ca) for pSPDir. In the absence of transpososome assembly, the Cre reactions yielded almost exclusively topologically simple products: the unknotted inversion product that comigrated with the substrate in pSPIn reactions (lane 2, Figure 3A), or the unlinked deletion circles (del1 and del2) in the pSPDir reactions (lane 2, Figure 3B).

The faint, unlabeled bands in lanes 4 and 6 in Figure 3 are the result of a weak DNA nicking activity present under these conditions, causing the recombination products to be relaxed (see below). Under our assay conditions, Cre recombined roughly 40%–60% of the input pSPIn and pSPDir plasmids. The reaction mixtures subjected to Cre recombination (lanes 2, 4, and 6) were deproteinized prior to electrophoresis. Hence, the absence in lanes 6 (Figures 3A and 3B) of the band corresponding to the fraction of the type 0 complex that was not recombined by Cre. Following dissociation, the type 0 complex would migrate at the position of the supercoiled form of the substrate.

Products of Cre Recombination from the LER-Cre or Type 0-Cre Synapses Are Topologically Unique

The contrasting outcomes of Cre recombination from its native synapse and the hybrid synapses (LER-Cre or type 0-Cre) demonstrate that the Mu transpososome endows the Cre reaction with topological attributes that it normally lacks. The product topologies of the reactions shown in lanes 4 and 6 of Figures 3A and 3B were probed by DNase I nicking and subsequent fractionation by gel electrophoresis and by electron microscopy (Figures 4A and 4B). For the Cre alone reaction with pSPIn (from lane 2, Figure 3A), essentially all of the nicked products comigrated with the nicked substrate as predicted for the unknotted recombinant (lane 2, Figure 4A). Diagnostic restriction enzyme digestions of DNA isolated from this band revealed the coexistence of the parental and recombined forms of pSPIn within it (results not shown). In the Cre reactions from the LER and type 0 complexes (from lanes 4 and 6, Figure 3A), a species migrating with the mobility of the trefoil knot (as measured against a knot ladder; see Experimental Procedures) was the predominant product, together with a minor species migrating as the pentafoil knot (lanes 3 and 4, Figure 4A). Electron microscopy confirmed this inference, and revealed the sign of the knot crossings in the trefoil to be exclusively + (right panel, Figure 4A). For pSPDir (from lane 2, Figure 3B), Cre by itself gave almost exclusively unlinked deletion circles along with a trace of the 2-noded catenane (lane 2, Figure 4B; the smaller of the circles del1 had migrated out of the gel). By contrast, the Cre reactions subsequent to LER and type 0 assembly (from lanes 4 and 6, Figure 3B) caused a marked enrichment in the yield of the 4-noded catenane (lanes 3 and 4, Figure 4B). Electron microscopy established these catenanes to be exclusively right-handed (right panel, Figure 4B). The uncatenated deletion circles (del2) in lane 3 (Figure 4B) denote the fraction of pSPDir that was not converted into the LER complex and/or the fraction of LER that dissociated during the Cre reaction.

Not only does the LER and type 0 synapse confer topological complexity on the Cre recombination reaction but also topological uniqueness, as revealed by the predominant production of the trefoil during inversion and the 4-noded catenane during deletion. Among more than 50 clearly discernible trefoils scored by electron microscopy, every one was of the + crossing type; similarly, all of the >20 catenanes examined were of the right-handed variety. This unique product topology, in turn, reflects the unique topology of the LER and type 0 synapses. The identity of the products from the LER-Cre and type 0-Cre synapses attests to the topological equivalence between LER and type 0 in the interaction of the enhancer with the att sites.

The Enhancer Crosses the attL and attR DNA Thrice within the LER and Type 0 Synapses

The formation of +3 trefoils and right handed 4-noded catenanes during MuA-assisted Cre recombination implies that the LER and type 0 synapses precisely sequester three plectonemic negative supercoil nodes as a consequence of the enhancer crossing the attL-attR sites. The small fraction of pentafoils populating the inversion product (lanes 3 and 4, Figure 4A) can be accounted for by the occasional entrapment of a random supercoil. Pentafoil formation from a small fraction of the Mu synapse that contains four crossings between the enhancer and att sites is unlikely, but cannot be ruled out entirely. Neither explanation undermines our main conclusions.

In pSPIn, the three nodes (or an odd number of nodes) would impose antiparallel geometry on the *loxP* sites. In the trefoil product of recombination, the node signs are changed from – to + because of the relative inversion of the DNA segment between the two *loxP* sites. In pSPDir, Cre must utilize a fourth supercoil node (a final tally of an even number of nodes) to correctly align the *loxP* partners. The product circles resulting from recombination will therefore be interlinked via four negative crossings. The +3 trefoils could, in principle, have resulted from 2 supercoils trapped by the Mu synapse and the third introduced by Cre for the antiparallel arrangement of the head to head *loxP* sites of pSPIn. We can rule out this possibility because the corresponding catenane product from pSPDir should have been a 2-noded catenane and not a 4-noded catenane (as observed here).

The overall efficiencies of Cre recombination after the assembly of the LER or type 0 synapse were not significantly different for the pSPIn and pSPDir substrates. This can be seen by comparing the intensities of the type 0 and the corresponding Kn(sc) and Ca(sc) bands in lanes 5 and 6 of Figures 3A and 3B. The energetic cost of trapping a fourth node, once the −3 crossing synapse has been preestablished, for the deletion reaction in negatively supercoiled pSPDir, would be minimal. Hence, the rough equivalence in the extent of deletion in pSPDir to that of inversion in pSPIn in the MuA/HU-assisted Cre reactions. In the unassisted Cre reactions, the yield of deletion from pSPDir was approximately 15%–20% higher than that of inversion from pSPIn (data not shown).

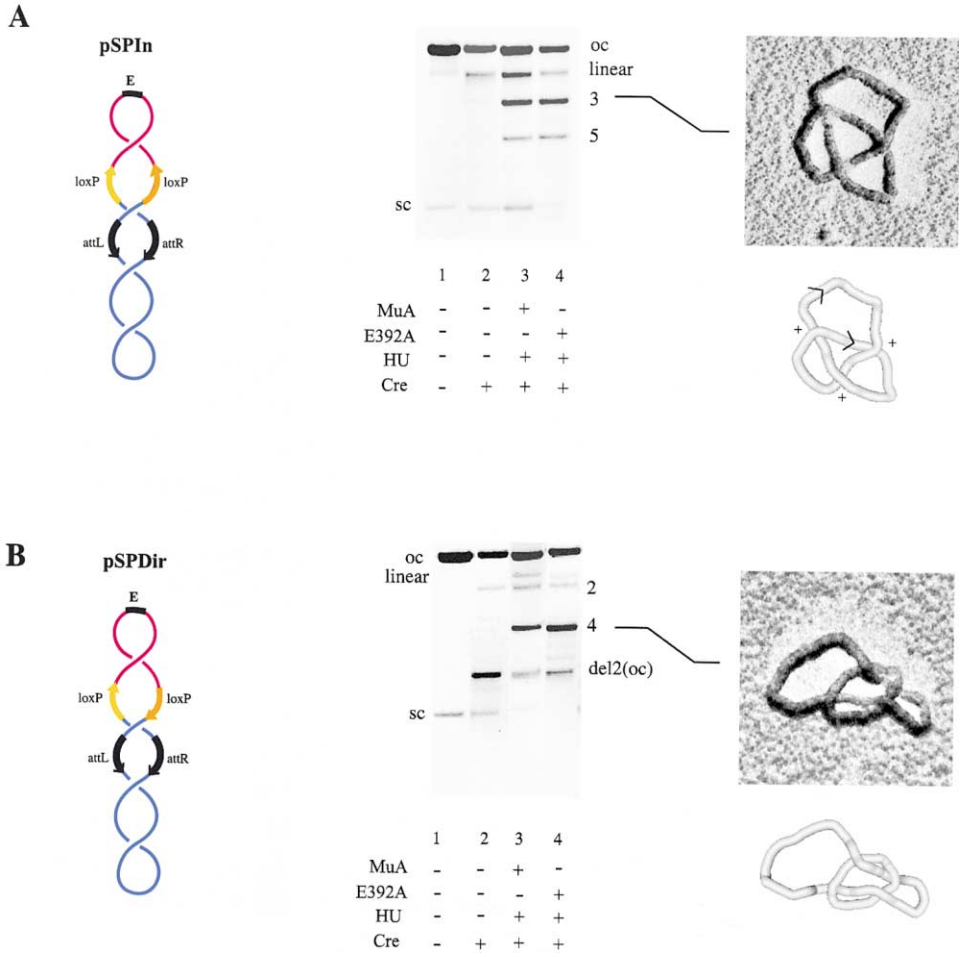

Figure 4. Topological Analysis of Cre Recombination Products Formed from the Native and Hybrid Synapses

(A and B) Reactions corresponding to lanes 2, 4, and 6 of Figures 3A and 3B were nicked with DNase I and analyzed by agarose gel electrophoresis. In both (A) and (B), lane 1, substrate alone; lane 2, Cre alone reaction; lane 3, Cre/LER reaction; and lane 4, Cre/type 0 reaction. The representative electron micrographs shown here were obtained from the Cre/type 0 reaction with pSPIn substrates (A, lane 4), and the Cre/LER reaction with pSPDir (B, lane 3). The trefoils harbor + DNA crossings and the catenanes are right handed as per standard conventions (White and Cozzarelli, 1984).

The Unique Topology of the Mu Synapse Is Absolutely Dependent on the Enhancer

In order to ascertain the role of the enhancer in the topology of the Mu synapse, the Cre recombination reactions were carried out in plasmids that are similar to pSPIn and pSPDir in the organization and relative orientations of attL, attR, and *loxP* sequences, but lack the enhancer element. Reactions with these plasmids, pSPIn(ΔEn) and pSPDir(ΔEn), gave identical results with both MuA and MuA(E392A). The data shown in Figures 5A and 5B correspond to assays performed with MuA(E392A). No type 0 complex was observed with either of the two plasmids, as indicated by the absence of a DNA species migrating just above their supercoiled forms in lane 3 of both Figures 5A and 5B. Similarly, the inversion and deletion reactions with Cre did not give topologically distinct products, depending on whether or not the plasmids were preincubated with MuA(E392A) and HU (compare lanes 2 and 4 in Figures 5A and 5B). Digestion of a reaction mixture equivalent to that in lane 4 of Figure 5A with BglII and HindIII confirmed inversion by Cre, as certified by the presence of the parental and recombinant bands, P and R, respectively (lane 5, Figure 5A). The deletion reactions by Cre with or without preincubation with MuA(E392A) and HU gave only uncatenated deletion circles (lanes 2 and 4, Figure 5B).

The results from plasmids lacking the enhancer demonstrate that the characteristic topology of the recombination products is directly derived from the Mu end-enhancer interactions mediated by MuA. We have further verified that the absence of DNA supercoiling, the attR element, or the HU protein, or the replacement of MuA or MuA(E392A) by derivatives lacking the enhancer binding domain abolishes the distinct Cre inversion and deletion products obtained. Details of these assays will be described elsewhere (S.P. et al., unpublished data).

Topological Outcomes of Cre Recombination when the *loxP* Sites Demarcate the attL Domain from the Enhancer-attR Domain

The complete topology of the Mu transpososome must include, in addition to the three crossings the enhancer

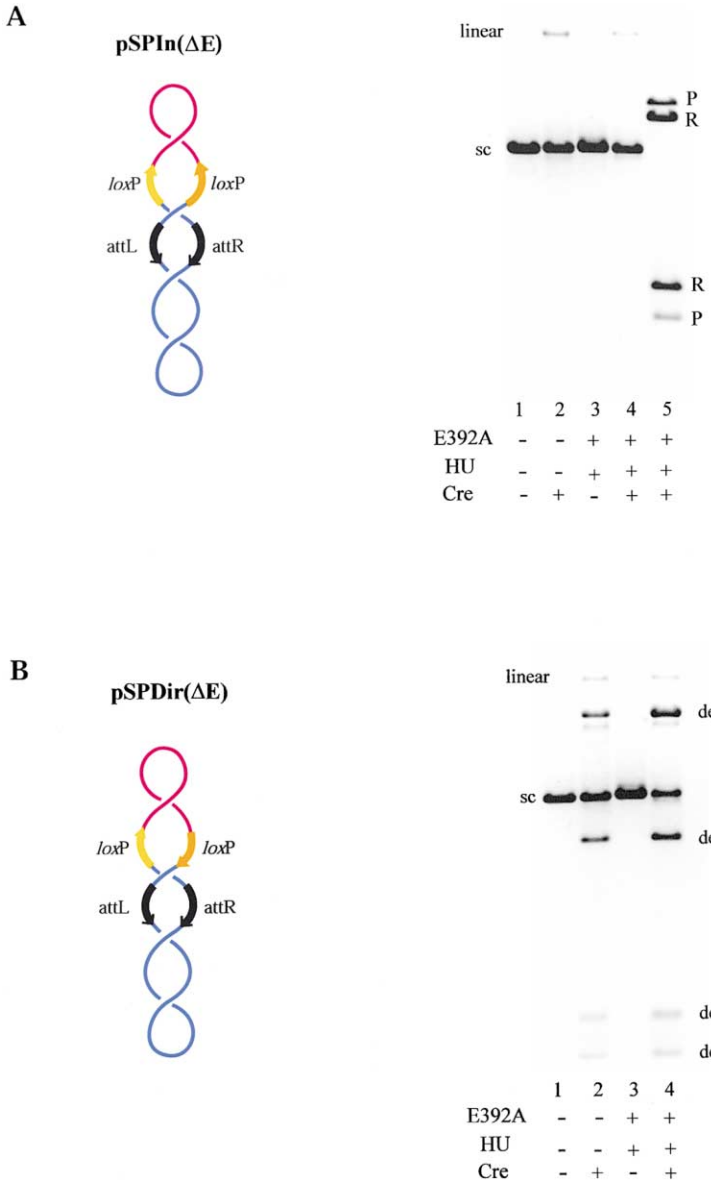

Figure 5. Effect of Enhancer Deletion on the Topology of the Cre Recombination Products

Type 0 assembly and Cre recombination were done as in the assays shown in Figure 3. (A) and (B) present the results with the inversion and deletion plasmids, respectively. The bands in lane 5 labeled P and R are the products resulting from HindIII-BglII digestion of the parental and recombined plasmids, respectively.

makes with the att sites (inferred from the data in Figure 4), potential crossings between attL and attR as well. We therefore wished to derive the number of attL-attR crossings by difference topology, while at the same time verifying the validity of the three-crossing interaction between the enhancer and the att sites. We also wished to determine how the three enhancer crossings are distributed between attL and attR. In the experiments represented in Figure 6, we have broken down the topology of the type 0 synapse into a series of subtopologies by sequentially partitioning attL and attR from each other and the enhancer using the *loxP* barriers (Figure 6).

In the assays shown in Figures 6A and 6B, we isolated the attL domain from the enhancer-attR domain by placing the *loxP* sites close to the termini of attL. The plasmids pSP(L)In and pSP(L)Dir (Figures 6A and 6B, respectively) were nearly identical in their organization, except for the relative orientation of the *loxP* sites. The *loxP* spacings with respect to the L3-proximal and L1-proximal ends of attL (see Figure 1B) were as follows: 139 bp and 105 bp in pSP(L)In; and 139 bp and 149 bp in pSP(L)Dir. Note that the pSP(L) plasmids, by segregating the attL domain from the attR-enhancer domain, will reveal the DNA crossings that attR and enhancer together make with attL.

The type 0 complex was preassembled with Mu-A(E392A) and HU, and recombination reactions were performed as described for the assays in Figure 3. For simplicity, only data from the DNase I-nicked reactions are shown in Figure 6. The yields of type 0 in these reactions were comparable to those in Figure 3; the levels of Cre recombination within preformed type 0, as judged by the amount of product migrating faster than the supercoiled substrate, were also similar.

As observed previously, the Cre alone reaction resulted almost exclusively in unknotted inversion product comigrating with the nicked substrate (lane 2 of Figure 6A) or unlinked deletion circles (lane 2 of Figure 6B; the

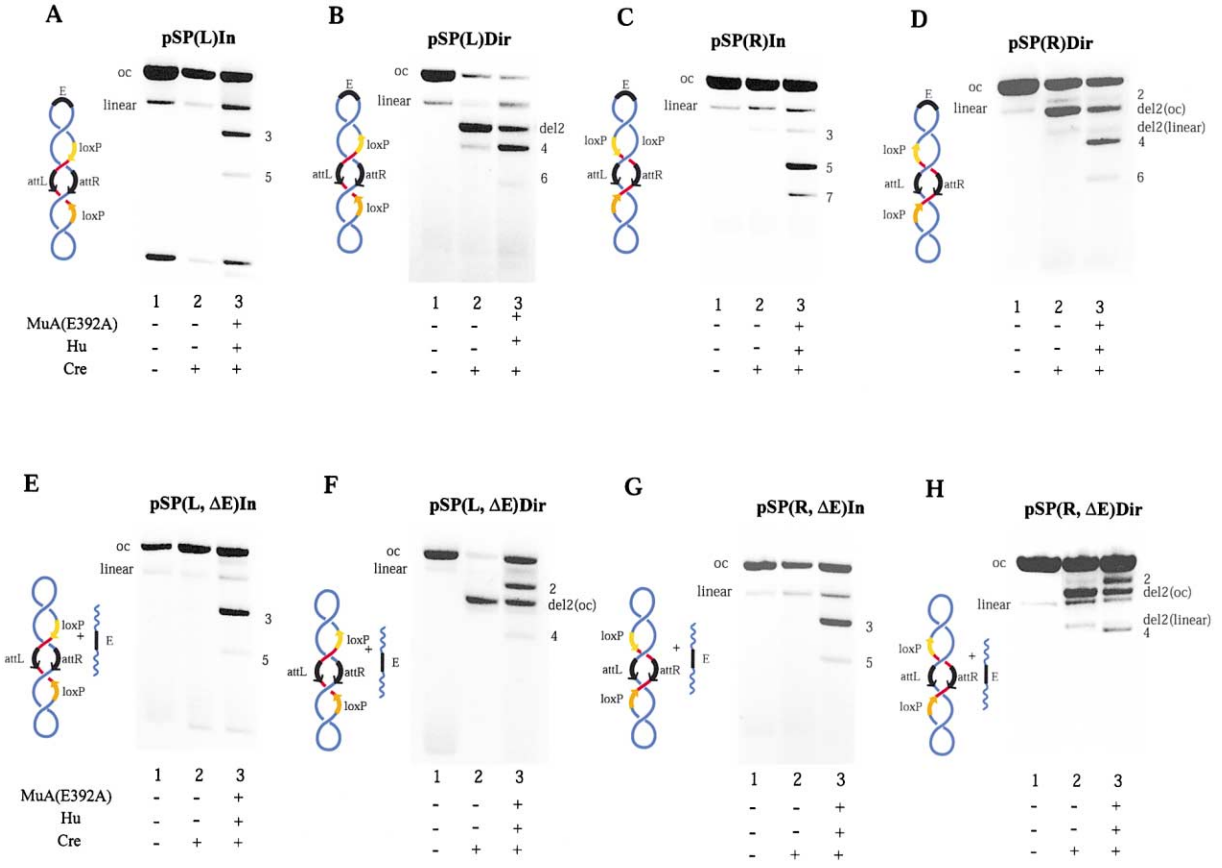

Figure 6. Topologies of the Type 0 Complexes Assembled with the Enhancer Provided in *cis* or in *trans*

In (A)–(D), the enhancer was present in *cis*; in (E–H), the enhancer was supplied in *trans*. In (A) and (B), attL was isolated from enhancer and attR. In (C) and (D), attR was isolated from enhancer and attL. In (E)–(H), attL and attR were segregated from each other. In each case, *loxP* sites marked domain borders. Products of Cre recombination in the absence of or following type 0 assembly were analyzed by DNase I nicking and gel electrophoresis.

smaller product del1 had run out of the gel). For the pSP(L)In and pSP(L)Dir plasmids, Cre inversion and deletion reactions following assembly of the type 0 complex caused the specific enrichment of the 3-noded knot and the 4-noded catenane, respectively (lane 3 in both Figures 6A and 6B). The product topologies thus assign three crossings between attL on the one hand and attR-enhancer on the other. Cre inversion converts them into a trefoil knot; Cre deletion, after aligning correctly the *loxP* sites with a fourth crossing, gives the 4-noded catenane.

Products of Cre Recombination when the attR Domain Is Quarantined from the attL-Enhancer Domain

The reactions in Figures 6C and 6D were analogous to those in Figures 6A and 6B, respectively. However, it was the attR domain that was segregated from the enhancer-attL domain by *loxP* sites positioned close to the termini of attR. The *loxP* distances from the R3-proximal and R1-proximal ends of attR (see Figure 1B) were as follows: 120 bp and 85 bp in pSP(R)In; and 120 bp and 100 bp in pSP(R)Dir. The design of the pSP(R) plasmids was suitable for extracting the number of DNA crossings that attR makes with attL and the enhancer.

Cre inversion and deletion reactions carried out after assembling the type 0 complex in the pSP(R) plasmids gave the 5-noded knot and the 4-noded catenane, respectively, as the specific enrichment products (lane 3 in both Figures 6C and 6D). These topological outcomes correspond to a total of four DNA crossings between attR on the one hand and attL-enhancer on the other.

Topological Outcomes of Cre Recombination from a Type 0 Complex Assembled by Providing the Enhancer in *trans*

Although the normal assembly of the Mu transpososome utilizes the enhancer in *cis*, it is nevertheless possible to support active transpososome formation by providing the enhancer in *trans* at high concentrations (Surette and Chaconas, 1992). We reasoned that, by repeating the assays shown in Figures 6A–6D with the enhancer supplied in *trans*, we could exclude its contribution to the topology of the Cre recombination from the type 0-Cre synapse. We can thus derive the DNA crossing number between attL and attR in the type 0 complex.

The plasmid substrates pSP(L,ΔE)In and pSP(L,ΔE)Dir were similar to their counterparts used in the experiments in Figures 6A and 6B in the relative organizations of the attL, attR, and *loxP* sites. They differed from the

latter in lacking the enhancer, as indicated by the ΔE symbol. Similarly, the plasmids pSP(R,ΔE)In and pSP(R,ΔE)Dir were the enhancerless derivatives of pSP(R)In and pSP(R)Dir (see Figures 6C and 6D). During type 0 assembly, the enhancer was supplied in the form of a 172 bp DNA fragment, obtained by PCR amplification, at a 50-fold higher molar concentration relative to attL or attR.

The profiles from the DNase I nicked reactions show that for pSP(L,ΔE)In, the product of Cre inversion from the type 0 complex was the trefoil knot (lane 3 of Figure 6E). Similarly, the outcome of the Cre deletion reaction from the type 0 complex formed by pSP(L,ΔE)Dir was the 2-noded catenane (lane 3 of Figure 6F). As was observed in all the other assays, the Cre alone reactions resulted in the unknotted inversion product overlapping with the substrate band (lane 2 of Figure 6E) or the unlinked deletion circle (lane 2 of Figure 6F). The products of Cre recombination carried out after enhancer-in-*trans* type 0 assembly were the trefoil knot for pSP(R,ΔE)In (lane 3 of Figure 6G) and the 2-noded catenane for pSP(R,ΔE)Dir (lane 3 of Figure 6H).

Thus, when the enhancer is topologically unlinked from the type 0 complex, the number of DNA nodes within it due to the crossings between attL and attR is two. The Cre deletion reaction from this two-crossing synapse would give the 2-noded catenane, as seen here with pSP(L,ΔE)Dir and pSP(R,ΔE)Dir. The Cre reactions from the type 0 complex formed by pSP(L,ΔE)In and pSP(R,ΔE)In would require a third node to orient the *loxP* sites correctly, and thus result in the 3-noded knot.

Discussion

The Type 0 Mu Transpososome Is a Five-Noded Synapse

In this study, we have carried out a complete topological anlaysis of the type 0 synapse and a partial analysis of the LER synapse formed during phage Mu transposition. For this purpose, the transpososome synapse was first divided into a set of sub-synapses in which the relevant DNA components were separated by *loxP* sites into binary domains. For every case, the topology was unambiguously determined by probing the Cre recombination outcome from a pair of matched inversion and deletion substrates. If a synapse has an odd number of crossings, this number will be declared by the DNA crossings in the knot product from the inversion substrate; and the linked product circles from the corresponding deletion substrate will contain one more DNA crossing. For an even noded synapse, the number of interlinks between the deletion circles will define the number of the synaptic nodes; and the corresponding inversion knot will contain one extra node. Each sub-synapse is thus characterized by the simpler of the two product topologies yielded by the paired inversion and deletion substrates used to unveil it (see below and Figure 7B).

In Figure 7A, we have represented the arrangements of attL, attR, and the enhancer within the type 0 complex that is consistent with the cumulative topological outcomes. A total of five negative supercoils are partitioned into the Mu transpososome. Of these, three represent crossings between the enhancer and attL-attR (results from Figures 3 and 4; see also Figure 7B-1), and two represent crossings between attL and attR (data from Figures 6E–6H; see also Figures 7B-2 and 7B-3). The three crossings between the enhancer and att DNA also hold true for the LER complex (data from Figures 3 and 4). Further dissection of the sub-topologies of the LER synapse by strategies analogous to those used for the type 0 analysis is presently being done.

The representation of the type 0 synapse (Figure 7A) shows that the three-crossing pattern between the enhancer and att DNA is partitioned 1 to 2 between attL and attR, respectively. This follows from the findings that attL thrice crosses the enhancer and attR together, and attR crosses four times the enhancer and attL together (data from Figures 6A–6D; see also Figures 7B-4 and 7B-5). Subtracting the two crossings between attL and attR (Figures 6E–6H; Figures 7B-2 and 7B-3) leaves one crossing ($3 - 2 = 1$) between the enhancer and attL and two crossings between the enhancer and attR ($4 - 2 = 2$).

"Criss-Crossed" Interactions between the Enhancer and the att-Sites

The enhancer overlaps with the Mu operator sites O1-O3, with O1 and O2 providing the minimal enhancer function (Chaconas and Harshey, 2002). Experiments using two transposase proteins (MuA and D108A) that share the same att specificity but have distinct enhancer specificities in conjunction with hybrid enhancers suggest that O1 functionally interacts with the R1 sub-site of attR, and O2 with the L1 subsite of attL. The interaction between O1-R1 is functionally dominant over that between O2 and L1 (Jiang et al., 1999). Since O1 is physically proximal to attL and O2 to attR, the enhancer-att interaction was referred to as criss-crossed. The spatial dispositions of O1, R1, O2, and L1 within the type 0 synapse diagrammed in Figure 7A are consistent with the deduced O1-R1 and O2-L1 interactions. The mutational studies of Allison and Chaconas (1992) indicate that O1-R2, O2-R3, and O1-L3 interactions are also important in the assembly of the Mu transpososome. These interactions can also be accommodated by the five-noded synapse. It is possible that all of the mapped interactions are not contemporaneous, and not all of them are necessarily retained in the mature transpososome. Nevertheless, the overall agreement between type 0 topology and the proposed att-enhancer interactions is satisfying.

Recent experiments (Jiang and Harshey, 2001) have shown that the O1-R1 and O2-L1 rules are obeyed even when the transpososome is assembled by providing the enhancer in *trans*. The enhancer acting in *trans* does not relax the requirement for the att sites to be in inverted orientation, nor does it exempt the transposition substrate from being negatively supercoiled. These findings allay the concern that the method of deriving attL and attR crossings by the enhancer-in-*trans* assay may not be valid. The interwrapping of the att sites, between themselves and with the enhancer in the type 0 complex explains at least in part why DNA supercoiling is required for transposition. Similarly, the topology of enhancer-att crossings (the enhancer is wound once around attL and twice around attR), together with the O1-R1 and O2-

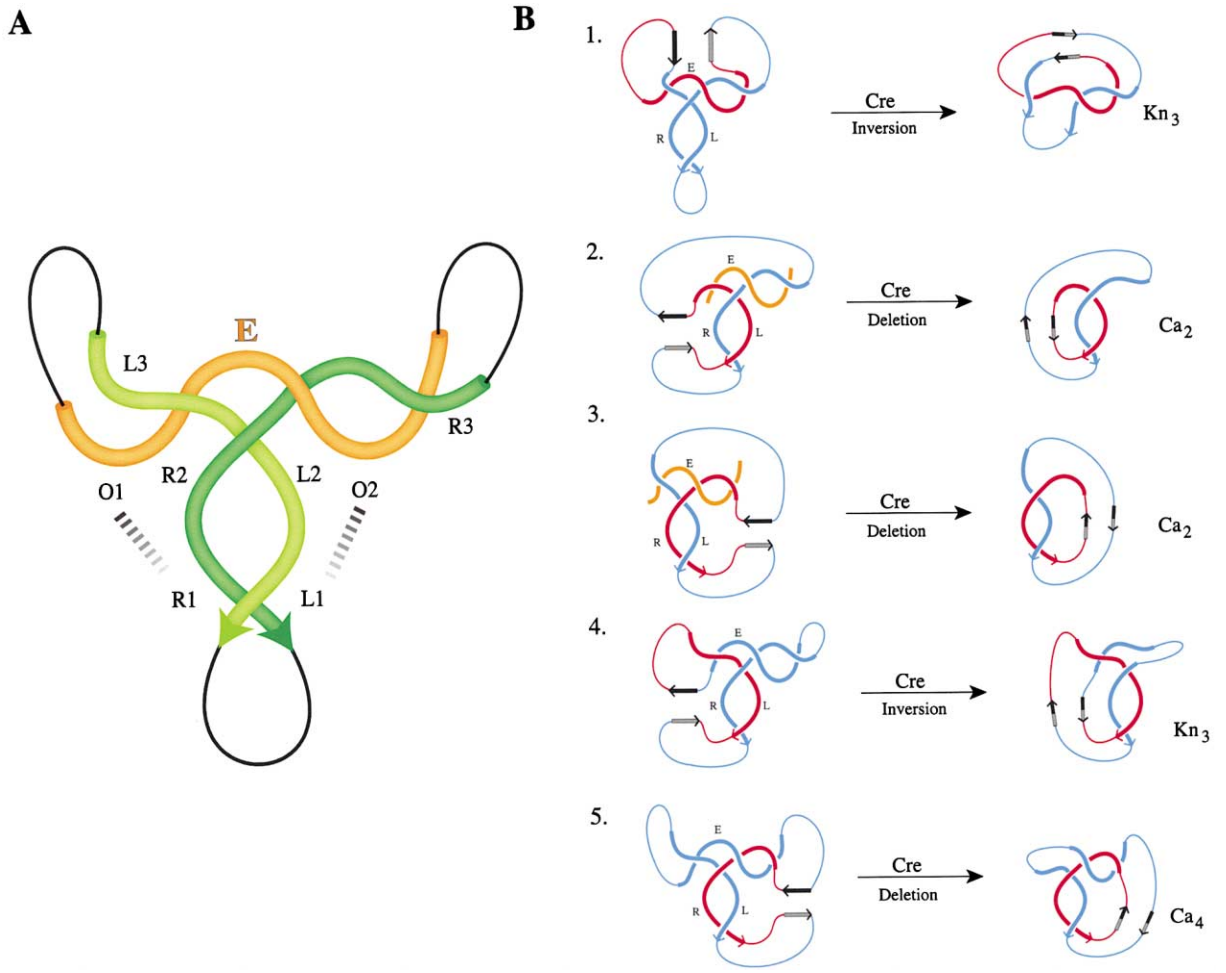

Figure 7. DNA Topology within the Mu Transposition Synapse

(A) shows the type 0 synapse with five trapped negative supercoil nodes. The attL, attR, and enhancer sites are color coded pale green, dark green, and gold, respectively. L1-L3 and R1-R3 refer to subsites within attL and attR, respectively. O1 and O2 are two of the operator sites within the enhancer (see Figure 1).

(B) shows the experimentally determined sub-topologies from which the composite topology in (A) was reconstructed. 1–5 depict the simpler of two product topologies yielded by the paired inversion and deletion substrates (Figures 3–6). In each case, the interacting sites are segregated into two domains (red and blue) with the *loxP* sites (black and gray arrows) marking the red-blue junctions. The domain demarcation is between enhancer and attL-attR in 1, between attL and attR in 2 and 3 (with enhancer, shown in gold, supplied in *trans*), between attL and enhancer-attR in 4, and between attR and enhancer-attL in 5. Exchange of DNA at the *loxP* sites traps three interdomainal (red × blue) crossings in 1, two in 2 and 3, three in 4, and four in 5.

L1 rule, can account for why the transposition enhancer, unlike classical transcription enhancers, is not orientation-independent (Leung et al., 1989; Mizuuchi and Mizuuchi, 1989).

Enhancer Association with the Type 0 Complex: Is It Really Transient?

The three-crossing enhancer-att interaction in both the LER and type 0 complexes calls for a rethinking of the generally accepted view that the enhancer is let go prior to type 0 assembly (see Figure 1A). According to our results, at the time the enhancer and att DNA domains are closed by the Cre synapse, the enhancer is still associated with the type 0 complex. In our assays, Cre was added to the reaction mixtures 20 min into the incubation of the substrate plasmids with MuA(E392A) and HU proteins at 30°C. Under these conditions, formation of the type 0 complex was completed in less than 10 min.

How do we reconcile our results with previous data suggesting that the enhancer makes its exit from the type 0 complex, as soon as it is assembled? It is clear that the enhancer is not required for the chemical steps of strand cleavage and strand transfer during Mu transposition. A type 0 complex, organized by supplying a linear enhancer in *trans*, is able to carry out DNA cleavage when supplied with Mg^{2+}, even though the enhancer is no longer associated with it (Surette and Chaconas, 1992). Mizuuchi et al. (1992) showed that binding of the Mu repressor to the enhancer (present, in this case, in *cis* with respect to attL and attR) blocks type 0 assembly. However, addition of repressor after completion of the assembly does not affect DNA cleavage in the presence of Mg^{2+} (Mizuuchi et al., 1992). The enhancer DNA in

the type 0 complex is still bound by the added repressor, as revealed by nuclease footprinting. Similarly, glutaraldehyde crosslinking followed by electron microscopy shows three DNA loops, indicative of enhancer association with the Mu ends in the LER complex but not in the type 0 complex (Watson and Chaconas, 1996).

The earlier biochemical results pose no conflict with the present topological data, provided the enhancer interacts with the type 0 synapse in a manner that freezes three supercoils, but is not itself topologically restrained within the synapse. In our assays, it is the Cre synapse, and not necessarily the Mu synapse, that would entrap the enhancer by closing DNA domains. It is possible that chemical crosslinking of the MuA tetramer, agarose gel electrophoresis, or nuclease nicking of DNA employed in previous experiments is responsible for releasing the enhancer from its association with the type 0 complex. Destabilization of the type 0 complex by nuclease nicking has been demonstrated (Mizuuchi et al., 1992; Wang et al., 1996). Furthermore, when electrophoresis is carried out in the absence of cross-linking, association of the enhancer with the Mu ends can be detected in a fraction of the type 0 population, when complexes are assembled under LER conditions (K. Kobryn and G. Chaconas, personal communication). The noninvasive nature of the Cre recombination assay employed in the present study has apparently preserved the fragile end-enhancer interactions, and allowed us to detect them from the topology of the recombinant products.

Recombinational enhancers not only assist in organizing a unique synapse (see citations in Jiang and Harshey, 2001), but are also implicated in modulating the conformation of the recombinase via directed protein-protein interactions (Klippel et al., 1993; Yang et al., 1995). Is the continued presence of the enhancer at the site of recombination necessary, or can it exit the complex after a functional synapse has been assembled? Topological experiments with the two related site-specific recombination systems (Gin and Hin), have produced opposite conclusions. The enhancer in the Gin system appears to be required only at the precatalytic step (Kanaar et al., 1990), whereas the enhancer in the Hin system apparently remains associated with the recombination complex during the chemical steps (Heichman et al., 1991). While the three crossings made by the Mu enhancer with the L and R ends may favor its continued presence within the type 0 synapse, the functional significance of its persistence as indicated in this study is not entirely clear. It could have subtle effects on the reaction in vivo, such as blocking the repressor from binding to the operators, or facilitating transposition immunity by directing integration events to outside the Mu domain. We are now assaying Cre recombination from preformed type I and type II complexes to ascertain the topological freedom (or lack thereof) of the enhancer upon completion of the strand cleavage and strand transfer reactions by the MuA tetramer.

Prospects

Uncovering functionally relevant architectural features of macromolecular assemblies containing multiple protein and nucleic acid components is a thorny general problem. The present work highlights the power of difference topology in tackling this challenge by revealing the DNA organization within a complex nucleoprotein arrangement designed to carry out DNA transposition. The analysis further suggests that even a labyrinthine DNA path involving multiple distant sites may be deciphered by first simplifying it into its constituent topologies contributed by a series of binary domains and subsequently superposing them to obtain the integrated topology.

Experimental Procedures

Plasmids

One copy each of the *lox*P site (Kilbride et al., 1999), 5′-ATAACTTCG TATAATGTATGCTATACGAAGTTAT-3′/3′-TATTGAAGCATATTAC ATACGATATGCTTCAATA-5′, was cloned into the NsiI and PstI sites in a derivative of plasmid pMK21, which contains the Mu attL and attR sites and the enhancer element (Kim et al., 1995). The NsiI site was placed 98 bp away from attL by PCR-based protocols. The *lox*P orientations at the NsiI site are opposite to each other in pSPIn and pSPDir; the orientations are the same at the PstI site. The plasmid pSPDir(ΔE) was obtained by deletion/substitution of the enhancer fragment of pSPDir, thus retaining the same relative distance between the *lox*P sites. One of the *lox*P sites on pSPDir(ΔE) was then inverted to give pSPIn(ΔE). The pSP(L)Dir plasmid was constructed by introducing *loxP* sites at NsiI and XbaI sites flanking attL. The *loxP* at XbaI was inverted in pSP(L)In. pSP(R)Dir and pSP(R)In were similarly constructed by introducing *loxP* at PstI and AatII sites flanking attR. The corresponding enhancerless variants (pSP(L,ΔE)In, pSP(L,ΔE)Dir, pSP(R,ΔE)In, and pSP(R,ΔE)Dir) were obtained by strategies analogous to those employed to construct pSPIn(ΔE) and pSPDir(ΔE).

Proteins

MuA, MuA(E392A), and *E. coli* HU proteins were purified as described by Yang et al. (1995). Cre protein was obtained as described in Grainge et al. (2000). IHF was a generous gift from S.Goodman, University of Southern California.

Mu Transposition Complexes and Cre Recombination Reactions

Type 0 and LER complexes were assembled at pH 7.6 (20 mM HEPES-KOH) using published protocols (Jiang and Harshey, 2001; Surette and Chaconas, 1992). In some assays, the enhancer (O1-O2) was supplied as a DNA fragment in *trans* in 50-fold molar excess of the plasmid substrate. These reactions included the *E. coli* IHF protein at a molar ratio of enhancer to IHF = 1:1.6. The type 0 or LER assembly time was 20 min for enhancer in *cis*, and 30 min for enhancer in *trans*, at 30°C. Cre reactions were incubated for 20 min at 30°C. Samples were processed as described by Grainge et al. (2000).

Formation of the LER complex was confirmed by glutaraldehyde crosslinking (Watson and Chaconas, 1996). To visualize the type 0 complex, samples were heparin treated prior to electrophoresis (Kim et al., 1995). Preliminary assays indicated that the topologies of Cre recombination products (see Figure 3–6) were the same whether or not heparin challenge preceded the Cre reaction. However, the overall yield of the inversion or deletion products was reduced in the presence of heparin. The data presented in Figure 3–6 were obtained from recombination performed in the absence of heparin treatment.

To obtain marker knot and catenane ladders, Cre recombination was carried out at pH 9.0 (Kilbride et al., 1999).

Electron Microscopy

The nicked knots and catenanes were denatured to remove the nicked strand, coated with *E. coli* RecA protein, and viewed by electron microscopy with assistance from Nancy Crisona at UC Berkeley, CA. The details of the method have been described elsewhere (Zechiedrich and Crisona, 1999).

Acknowledgments

We thank Nancy Crisona and Nick Cozzarelli for teaching us the electron microscopy of RecA-coated DNA knots and catenanes, Steve Goodman for IHF protein, Ian Grainge for discussions, and Nick Cozzarelli, Arlen Johnson, and Alan Lambowitz for insightful comments on the manuscript. We acknowledge Kristina Schlegel for help with one of the figures. This work was funded by the National Institutes of Health (GM33247 to RMH and GM35654 to MJ), and in part by the Robert Welch Foundation (F-1351 to RMH and F-1274 to MJ).

Received: December 4, 2001
Revised: March 20, 2002

References

Allison, R.G., and Chaconas, G. (1992). Role of the A protein-binding sites in the in vitro transposition of Mu DNA. A complex circuit of interactions involving the Mu ends and the transpositional enhancer. J. Biol. Chem. *267*, 19963–19970.

Chaconas, G., and Harshey, R.M. (2002). Transposition of phage Mu DNA. In Mobile DNA II, N. Craig, A. Lambowitz, M. Gellert, and R. Craigie, eds. (Washington, DC: ASM Press), pp 384–402.

Chalmers, R., Guhathakurta, A., Benjamin, H., and Kleckner, N. (1998). IHF modulation of Tn10 transposition: sensory transduction of supercoiling status via a proposed protein/DNA molecular spring. Cell *93*, 897–908.

Colloms, S.D., Bath, J., and Sherratt, D.J. (1997). Topological selectivity in Xer site-specific recombination. Cell *88*, 855–864.

Grainge, I., Buck, D., and Jayaram, M. (2000). Geometry of site alignment during int family recombination: antiparallel synapsis by the Flp recombinase. J. Mol. Biol. *298*, 749–764.

Grindley, N.D.F. (1994). Resolvase-mediated site-specific recombination. In Nucleic Acids and Molecular Biology, F. Eckstein, and D.M.J. Lilley, eds. (Berlin: Springer-Verlag), pp. 236–267.

Guo, F., Gopaul, D.N., and van Duyne, G.D. (1997). Structure of Cre recombinase complexed with DNA in a site-specific recombination synapse. Nature *389*, 40–46.

Halford, S.E. (2001). Hopping, jumping, and looping by restriction enzymes. Biochem. Soc. Trans. *29*, 363–374.

Heichman, K.A., Moskowitz, I.P., and Johnson, R.C. (1991). Configuration of DNA strands and mechanism of strand exchange in the Hin invertasome as revealed by analysis of recombinant knots. Genes Dev. *5*, 1622–1634.

Hirano, T. (2000). Chromosome cohesion, condensation, and separation. Annu. Rev. Biochem. *69*, 115–144.

Holmes, V.F., and Cozzarelli, N.R. (2000). Closing the ring: links between SMC proteins and chromosome partitioning, condensation, and supercoiling. Proc. Natl. Acad. Sci. USA *97*, 1322–1324.

Jiang, H., and Harshey, R.M. (2001). The Mu enhancer is functionally asymmetric both in *cis* and in *trans*. Topological selectivity of Mu transposition is enhancer-independent. J. Biol. Chem. *276*, 4373–4381.

Jiang, H., Yang, J.Y., and Harshey, R.M. (1999). Criss-crossed interactions between the enhancer and the att sites of phage Mu during DNA transposition. EMBO J. *18*, 3845–3855.

Kanaar, R., Klippel, A., Shekhtman, E., Dungan, J.M., Kahmann, R., and Cozzarelli, N.R. (1990). Processive recombination by the phage Mu Gin system: implications for the mechanisms of DNA strand exchange, DNA site alignment, and enhancer action. Cell *62*, 353–366.

Kilbride, E., Boocock, M.R., and Stark, W.M. (1999). Topological selectivity of a hybrid site-specific recombination system with elements from Tn3 res/resolvase and bacteriophage P1 loxP/Cre. J. Mol. Biol. *289*, 1219–1230.

Kim, K., Namgoong, S.Y., Jayaram, M., and Harshey, R.M. (1995). Step-arrest mutants of phage Mu transposase. Implications in DNA-protein assembly, Mu end cleavage, and strand transfer. J. Biol. Chem. *270*, 1472–1479.

Klippel, A., Kanaar, R., Kahmann, R., and Cozzarelli, N.R. (1993). Analysis of strand exchange and DNA binding of enhancer-independent Gin recombinase mutants. EMBO J. *12*, 1047–1057.

Leung, P.C., Teplow, D.B., and Harshey, R.M. (1989). Interaction of distinct domains in Mu transposase with Mu DNA ends and an internal transpositional enhancer. Nature *338*, 656–658.

Matthews, K.S. (1992). DNA looping. Microbiol. Rev. *56*, 123–136.

Mizuuchi, K. (1992). Transpositional recombination: mechanistic insights from studies of Mu and other elements. Annu. Rev. Biochem. *61*, 1011–1051.

Mizuuchi, M., and Mizuuchi, K. (1989). Efficient Mu transposition requires interaction of transposase with a DNA sequence at the Mu operator: implications for regulation. Cell *58*, 399–408.

Mizuuchi, M., Baker, T.A., and Mizuuchi, K. (1992). Assembly of the active form of the transposase-Mu DNA complex: a critical control point in Mu transposition. Cell *70*, 303–311.

Ristic, D., Wyman, C., Paulusma, C., and Kanaar, R. (2001). The architecture of the human Rad54-DNA complex provides evidence for protein translocation along DNA. Proc. Natl. Acad. Sci. USA *98*, 8454–8460.

Schleif, R. (1992). DNA looping. Annu. Rev. Biochem. *61*, 199–223.

Stark, W.M., Boocock, M.R., and Sherratt, D.J. (1992). Catalysis by site-specific recombinases. Trends Genet. *8*, 432–439.

Surette, M.G., and Chaconas, G. (1992). The Mu transpositional enhancer can function in *trans*: requirement of the enhancer for synapsis but not strand cleavage. Cell *68*, 1101–1108.

Tahirov, T.H., Sato, K., Ichikawa-Iwata, E., Sasaki, M., Inoue-Bungo, T., Shiina, M., Kimura, K., Takata, S., Fujikawa, A., Morii, H., et al. (2002). Mechanism of c-Myb-C/EBP beta cooperation from separated sites on a promoter. Cell *108*, 57–70.

Tjian, R., and Maniatis, T. (1994). Transcriptional activation: a complex puzzle with few easy pieces. Cell *77*, 5–8.

Wang, Z., Namgoong, S.Y., Zhang, X., and Harshey, R.M. (1996). Kinetic and structural probing of the precleavage synaptic complex (type 0) formed during phage Mu transposition. Action of metal ions and reagents specific to single-stranded DNA. J. Biol. Chem. *271*, 9619–9626.

Wasserman, S.A., and Cozzarelli, N.R. (1985). Determination of the stereostructure of the product of Tn3 resolvase by a general method. Proc. Natl. Acad. Sci. USA *82*, 1079–1083.

Watson, M.A., and Chaconas, G. (1996). Three-site synapsis during Mu DNA transposition: a critical intermediate preceding engagement of the active site. Cell *85*, 435–445.

White, J.H., and Cozzarelli, N.R. (1984). A simple topological method for describing stereoisomers of DNA catenanes and knots. Proc. Natl. Acad. Sci. USA *81*, 3322–3326.

Yang, J.Y., Jayaram, M., and Harshey, R.M. (1995). Enhancer-independent variants of phage Mu transposase: enhancer-specific stimulation of catalytic activity by a partner transposase. Genes Dev. *9*, 2545–2555.

Zechiedrich, E.L., and Crisona, N.J. (1999). Coating DNA with RecA protein to distinguish DNA path by electron microscopy. In DNA Toposiomerase Protocols, M. Bjornsti, and N. Osheroff, eds. (Totowa, NJ: Humana Press), pp. 99–107.